NEOPLASIA
www.neoplasia.com

Volume 11 Number 12 December 2009 pp. 1371–1382 1371

Regulation of *Membrane-Type 4 Matrix Metalloproteinase* by SLUG Contributes to Hypoxia-Mediated Metastasis[1,2]

Chi-Hung Huang[*,†,3], Wen-Hao Yang[‡,3], Shyue-Yih Chang[§,¶], Shyh-Kuan Tai[‡,§,¶], Cheng-Hwei Tzeng[§,#], Jung-Yie Kao[†], Kou-Juey Wu[*,] and Muh-Hwa Yang[‡,#,**]**

*Institute of Biochemistry & Molecular Biology, National Yang-Ming University, Taipei 112, Taiwan; [†]Institute of Biochemistry, National Chung-Hsing University, Taichung 402, Taiwan; [‡]Institute of Clinical Medicine, National Yang-Ming University, Taipei 112, Taiwan; [§]Faculty of Medicine, National Yang-Ming University, Taipei 112, Taiwan; [¶]Department of Otolaryngology, Taipei Veterans General Hospital, Taipei 112, Taiwan; [#]Division of Hematology-Oncology, Department of Medicine, Taipei Veterans General Hospital, Taipei 112, Taiwan; **Genomic Research Center, Taipei Veterans General Hospital, Taipei 112, Taiwan

Abstract

The hypoxic tumor environment has been shown to be critical to cancer metastasis through the promotion of angiogenesis, induction of epithelial-mesenchymal transition (EMT), and acquisition of invasive potential. However, the impact of hypoxia on the expression profile of the proteolytic enzymes involved in invasiveness is relatively unknown. Membrane-type 4 matrix metalloproteinase (MT4-MMP) is a glycosyl-phosphatidyl inositol–anchored protease that has been shown to be overexpressed in human cancers. However, detailed mechanisms regarding the regulation and function of MT4-MMP expression in tumor cells remain unknown. Here, we demonstrate that hypoxia or overexpression of hypoxia-inducible factor-1α (HIF-1α) induced MT4-MMP expression in human cancer cells. Activation of SLUG, a transcriptional factor regulating the EMT process of human cancers, by HIF-1α was critical for the induction of MT4-MMP under hypoxia. SLUG regulated the transcription of *MT4-MMP* through direct binding to the E-box located in its proximal promoter. Short-interference RNA–mediated knockdown of MT4-MMP attenuated *in vitro* invasiveness and *in vivo* pulmonary colonization of tumor cells without affecting cell migratory ability. MT4-MMP promoted invasiveness and pulmonary colonization through modulation of the expression profile of MMPs and angiogenic factors. Finally, coexpression of HIF-1α and MT4-MMP in human head and neck cancer was predictive of a worse clinical outcome. These findings establish a novel signaling pathway for hypoxia-mediated metastasis and elucidate the underlying regulatory mechanism and functional significance of MT4-MMP in cancer metastasis.

Neoplasia (2009) 11, 1371–1382

Abbreviations: ChIP, chromatin immunoprecipitation; EMT, epithelial-mesenchymal transition; FBS, fetal bovine serum; HIF-1α, hypoxia-inducible factor-1; HNSCC, head and neck squamous cell carcinoma; ICC, immunocytochemistry; IHC, immunohistochemistry; MMP, matrix metalloproteinase; MT4-MMP, membrane-type 4 matrix metalloproteinase; ΔODD, oxygen degradation domain; siRNA, short-interference RNA

Address all correspondence to: Muh-Hwa Yang, MD, PhD, Institute of Clinical Medicine, National Yang-Ming University, No. 155, Sec. 2, Li-Nong St, Peitou, Taipei 112, Taiwan. E-mail: mhyang2@vghtpe.gov.tw or Kou-Juey Wu, MD, PhD, Institute of Biochemistry and Molecular Biology, National Yang-Ming University, No. 155, Sec. 2, Li-Nong St, Peitou, Taipei 112, Taiwan. E-mail: kjwu2@ym.edu.tw

[1]This work was supported in part by National Science Council grants 96-2314-B-075-013; 97-2314-B-010-003 (M.H.Y.), 97-2320-B-010-029 (K.J.W.) ,and 98-2314-B-075-033 (C.H.T.); National Research Program for Genomic Medicine grants DOH97-TD-G-111-038 and DOH98-TD-G-111-027 (K.J.W.); Taipei Veterans General Hospital grants VGH 97-C1-032 97-ER2-008, 98-C1-50, and 98-ER-008 (M.H.Y.); the Ministry of Education, Aim for the Top University Plan grants 97-A-C-T510 (M.H.Y.), 97-A-C-T509, and 97-A-C-D104 (K.J.W.); and National Health Research Institutes grant NHRI-EX-97-9611BI (K.J.W.).
[2]This article refers to supplementary materials, which are designated by Tables W1 and W2 and Figures W1 to W4 and are available online at www.neoplasia.com.
[3]These authors contributed equally to this work.
Received 6 August 2009; Revised 10 September 2009; Accepted 14 September 2009

DOI 10.1593/neo.91326

Introduction

Intratumoral hypoxia caused by rapid proliferation of tumor cells is one of the most important mechanisms promoting tumor aggressiveness, metastasis, and resistance to therapy [1–5]. Tumor cell responses to hypoxia are orchestrated in part through activation of the transcription factor hypoxia-inducible factor-1 (HIF-1) [1–4]. HIF-1 is a heterodimeric protein consisting of a constitutively expressed subunit, HIF-1β, and a hypoxia-inducible subunit, HIF-1α. Stabilization of the HIF-1 transcriptional complex under hypoxic conditions promotes cancer metastasis through three major mechanisms: promotion of angiogenesis, induction of tumor cell epithelial-mesenchymal transition (EMT), and activation/induction of proteolytic enzymes mediating tumor cell invasiveness [4]. The most well-characterized mechanism of hypoxia-induced metastasis is the activation of vascular endothelial growth factor (VEGF) by HIF-1 to promote angiogenesis [6,7]. Tumor hypoxia facilitates lymphatic metastasis through modification of the migration and invasion of lymphatic endothelial cells [5]. Increased HIF-1 activity can also induce EMT, a critical mechanism for promotion of cancer cell metastasis, through the activation of EMT regulators including SNAIL, SLUG (also known as Snail2), TWIST, ZEB1, or SIP1 [4,8–13]. Finally, HIF-1 contributes to the development of cancer cell invasiveness through activation of proteolytic enzymes involved in cellular invasiveness (e.g., cathepsin D, matrix metalloproteinase-2 [MMP-2], and urokinase plasminogen activator receptor) [14,15]. However, in comparison with the well-established mechanisms of hypoxia/HIF-1–induced angiogenesis and EMT, the hypoxia/HIF-1 signaling pathways that regulate the activation of proteolytic enzymes (i.e., the "degradome") are relatively unknown.

MMPs are a family of zinc-binding endopeptidases that degrade extracellular matrix components and modify the pericellular environment, thus playing a pivotal role in the regulation of cancer cell growth, tumor-associated angiogenesis, and cancer metastasis [16–19]. The MMP family of proteins includes both secreted and membrane-anchored (i.e., membrane-type MMP, MT-MMP) proteases, which have distinct functions in mediating cancer cell invasiveness [20]. Membrane-type 4 MMP (MT4-MMP, also known as MMP-17) is a member of the glycosyl-phosphatidyl inositol–anchored membrane-type MMP subgroup, which is structurally and functionally distant from other MT-MMPs [20,21]. The importance of MT4-MMP in human cancers has been suggested by previous studies, which reported that it is overexpressed in human breast cancer tissues [22,23], and overexpression of MT4-MMP accelerates the *in vivo* growth and promotes the metastasis of breast cancer cells through alteration of the tumor vascular architecture [23,24]. In comparison with the abundant information currently available on the regulation and function of other membrane-type MMPs, the mechanisms of MT4-MMP regulation and its function in cancer remain to be established.

In this report, we explored one possible mechanism of MT4-MMP regulation and its role in hypoxia-induced metastasis. SLUG, an EMT regulator that is induced by hypoxia/HIF-1, is shown to directly regulate the expression of MT4-MMP. We also demonstrate that MT4-MMP plays a significant role in hypoxia-mediated metastasis and is also an important prognostic indicator in patients with head and neck cancer.

Materials and Methods

Cell Culture and Oxygen Deprivation

The human hypopharyngeal squamous cell carcinoma cell line FADU, tongue squamous cell carcinoma cell lines SAS and OECM-1, and embryonic kidney 293T cell line were obtained from American Type Culture Collection (Manassas, VA). FADU cells were cultured in Roswell Park Memorial Institute (RPMI)-1640 medium with 10% heat-inactivated fetal bovine serum (FBS), whereas 293T, SAS, and OECM-1 cells were cultured in Dulbecco's modified Eagle's medium with 10% FBS. Oxygen deprivation was carried out in a 37°C incubator with 1% O_2, 5% CO_2, and 94% N_2 for 18 hours.

Plasmids Construction and Short-interference RNA Experiment

The pcDNA3-SNAIL, pFLAG-CMV, and pFLAG-TWIST plasmids were described [12]. The plasmids pHA-HIF-1α, pHA-HIF-1α(ΔODD), and pHA-HIF-1α(LCLL) were gifts from Dr. L.E. Huang (University of Utah) [25,26]. The plasmid pcDNA3–MT4-MMP was generated by insertion of a 1821-bp fragment of the full-length human *MT4-MMP* complementary DNA (cDNA) from the plasmid pBluescriptR-(MT4-MMP) (Invitrogen Corporation, Carlsbad, CA) into the *Bam*HI/*Eco*RI sites of the pcDNA3.1 vector. The plasmid pcDNA3-SLUG was generated by insertion of an 807-bp fragment of the full-length human *SLUG* cDNA from the plasmid pCMV-SPORT6-Snail2 (Genomic Center, National Yang-Ming University) into the *Bam*HI/*Eco*RI sites of the pcDNA3.1 vector.

For the short-interference RNA (siRNA) experiment, the plasmid pSUPER-HIF-1α-si has been previously described [13]. The plasmids pSUPER-SLUG-si and pSUPER–MT4-MMP-si were generated by inserting an oligonucleotide containing siRNA target sequences specific to *SLUG* or *MT4-MMP* into the pSUPER vector. A scrambled sequence with no significant homology to any mammalian gene sequence was cloned into the pSUPER vector (pSUPER-scr-si) as a control for the siRNA experiments as previously described [27]. The sequences of the oligonucleotides used to generate the siRNA constructs are listed in Table W1.

Protein Extraction and Western Blot Analysis

Protein extraction from cultured cells was performed as previously described [28]. The protein content was determined using the Bradford method (Bio-Rad Laboratories, Hercules, CA). For Western blot analysis, 50 μg of protein extract from each clone was loaded into sodium dodecyl sulfate–polyacrylamide gels, proteins were separated using electrophoresis, and the separated proteins were transferred to nitrocellulose filters. The filters were probed with the appropriate primary antibody. An anti-glyceraldehyde 3-phosphate dehydrogenase antibody was used as a loading control. Signals from bound antibodies were developed using an ECL chemiluminescence kit (Amersham Biosciences, London, UK). The characteristics of the antibodies used in the Western blot analyses are listed in Table W2.

RNA Extraction, Reverse Transcription, and Quantitative Real-time Polymerase Chain Reaction Analysis

Total RNA from cultivated cells were extracted using TRIzol reagent (Invitrogen Life Technologies). cDNA synthesis was performed as previously described [28]. To evaluate *HIF-1α* and *MT4-MMP* mRNA expression, quantitative real-time polymerase chain reaction (PCR) was performed using a PRISM7700 Sequence Detection System (Applied Biosystems, Foster City, CA) with the preset PCR program. Glyceraldehyde 3-phosphate dehydrogenase was selected as an internal control of each experiment. The primer sequences used in real-time PCR are presented in Table W1.

Cloning of the Human MT4-MMP and E-cadherin Promoter Region, Generation of MT4-MMP– and E-cadherin–driven Reporter Constructs, Transient Transfection, and Luciferase Assays

The genomic regions flanking the *MT4-MMP* gene promoter region (approximately −862 to +880 bp to ATG; Figure 4*A*) were generated by PCR amplification of human genomic DNA and inserted into the *Hin*dIII/*Bgl*II sites of the pXP2 vector to generate the MT4-Luc862 as a parietal construct. The ATG translation initiation codon of *MT4-MMP* was changed to CTG by site-directed mutagenesis to ensure translation of luciferase open reading frame of the MT4Luc862 construct. The MT4-Luc606, MT4-Luc433, MT4-Luc290, and MT4-Luc57 constructs were generated from MT4-Luc862 parietal construct for determining the putative regulatory region in *MT4-MMP* promoter. The MT4-Luc862Mut construct was generated by changing the sequence from CACCTG (approximately −462 to −457 bp to ATG) to AGAACT in MT4-Luc862 construct by site-directed mutagenesis (Figure 4*A*). The genomic regions flanking the *E-cadherin* gene promoter region containing E-boxes (approximately −486 to −79 bp to ATG; Figure 3*A*) were generated by PCR amplification of human genomic DNA and inserted into the *Hin*dIII/*Bgl*II sites of the pXP2 vector to generate the Ecad-Luc486.

The reporter constructs were cotransfected into 293T cells with pcDNA3-SNAIL, pcDNA3-SLUG, or pFLAG-TWIST and the internal control plasmid pcDNA3.1 or pFLAG-CMV under either normoxic or hypoxic conditions. A plasmid expressing the bacterial β-galactosidase gene (pCMV-βgal) was also cotransfected in each experiment as an internal control for transfection efficiency. Cells were harvested after 48 hours of transfection, and the luciferase activities were assayed as described [13]. All values are expressed as the fold change in luciferase activity after normalization using β-galactosidase activity.

Chromatin Immunoprecipitation

Chromatin immunoprecipitation (ChIP) assays were performed as previously described [13]. Briefly, cell lysates were incubated with no antibody, immunoglobulin G (IgG), or an antibody specific for SLUG. The experimental PCR reactions generated a 196-bp product from the regulatory region of the *MT4-MMP* gene containing an E-box, whereas the control PCR reactions generated a 146-bp product from a distal region without an E-box (Figure 4*C*, *upper panel*). The primers and antibodies used in the ChIP assays are listed in Tables W1 and W2.

Cell Migration and Invasiveness Assays

The Boyden chamber cell migration and invasion assays were performed as previously described [29]. All experiments used 8-μm pore size Boyden chambers. Briefly, cells (1×10^5) in medium containing 0.5% serum were seeded in the upper chamber, and 15% FBS was added to medium in the lower chamber as a chemoattractant. For invasion assays, the upper side of the filter was covered with Matrigel (Collaborative Research, Inc, Boston, MA). After 12 hours for migration assays or 24 hours for invasion assays, cells on the upper side of the filter were removed, and cells that remained adherent to the underside of membrane were fixed in 4% formaldehyde and stained with Hoechst 33342 dye. Ten contiguous fields of each sample were examined using a microscope and a 40× objective to obtain a representation of the number of cells that had invaded across the membrane.

In Vivo *Tail Vein Metastasis Assay*

Six-week-old female nonobese diabetic–severe combined immunodeficient (NOD-SCID) mice received injections of 1×10^6 cells of different clonal cell lines (SAS-cDNA3, SAS-HIF1α(ΔODD)-si-scr, SAS-HIF1α(ΔODD)-si-SLUG, SAS-HIF1α(ΔODD)-si–MT4-MMP, SAS-SLUG-si-scr, SAS-SLUG-si–MT4-MMP, and SAS–MT4-MMP) in 0.1 ml of PBS through the tail vein ($n = 6$ mice per group). Six weeks after injection, mice underwent gross examination and necropsy to assess the presence of metastases in the internal organs. Microscopic examination of metastases was performed on the cross sections of formalin-fixed, paraffin-embedded lung tissues stained with hematoxylin and eosin. The counting of metastatic lesions in the internal organ of each mouse was evaluated by gross and microscopic examination. This study was approved by the ethics committee of the Taipei Veterans General Hospital.

Study Population, Sample Collection, Immunohistochemistry, Validation of Antibodies, and Scoring

The records of sixty-eight patients with head and neck squamous cell carcinoma (HNSCC) who underwent treatment at Taipei Veterans General Hospital between January 2001 and December 2005 were retrospectively analyzed. This study was approved by the institutional review board of Taipei Veterans General Hospital. Patients' clinical characteristics are summarized in Table 1. Primary tumor samples and corresponding non-cancerous matched tissue were obtained for analysis during surgery. Fixed tissue processing through deparaffinization, rehydration, antigen retrieval, and immunohistochemistry (IHC) was performed as previously described [28,29]. To validate the HIF-1α and MT4-MMP antibodies used in IHC experiments, immunocytochemistry (ICC) of HIF-1α was performed in 293T cells under normoxia *versus* hypoxia, and ICC of MT4-MMP was performed in 293T cells transfected with control vector *versus* pcDNA3–MT4-MMP. Peptide blocking reagent without adding antibody was applied as the negative control of ICC experiments. The results showed that anti–HIF-1α antibody could detect HIF-1α located in the nucleus under hypoxia (Figure W4*A*), and the anti–MT4-MMP antibody

Table 1. Characteristics and Univariate Survival Analysis of 68 HNSCC Cases.

Variables	Case No.	Median OS (months)	*P*
Age (years)			.220
<50	28	—*	
≥50	40	22.6	
Sex			.588
Male	65	22.6	
Female	3	—*	
T stage			.026
1–2	30	—*	
3–4	38	18.0	
N stage			<.001
0	50	—*	
1-3	18	14.0	
HIF-1α overexpression			.006
Yes	28	14.0	
No	40	—*	
MT4-MMP overexpression			.081
Yes	37	18	
No	31	—*	
HIF-1α/MT4-MMP coexpression			.005
Yes	20	14.0	
No	48	—*	

OS indicates overall survival.
*Median survival was not reached.

could detect cytoplasmic MT4-MMP in MT4-MMP–overexpressing 293T cells (Figure W4*B*). All antibodies used for IHC are listed in Table W2.

HIF-1α and MT4-MMP IHC results were assessed independently by two specialists. HIF-1α immunoreactivity was interpreted as previously described [13], with greater than 50% nuclear staining scored as a positive result. MT4-MMP expression was scored with reference to other membrane-cytoplasmic proteins [28,29], with only appreciable staining distinctly marking the cytoplasm and/or nucleus, or dark staining completely obscuring the cytoplasm and/or nucleus in more than 25% of tumor cells considered as positive.

Statistical Analysis

An independent Student's *t*-test was used to compare continuous variables between two groups, and a χ^2 test was applied for comparison of dichotomous variables. A Kaplan-Meier estimate was used for survival analysis, and a log-rank test was used to compare the cumulative survival durations in the different patient groups. Unless otherwise specified in the figure legends, the control groups for all the statistical analyses were the first groups in the panels. Statistical significance was accepted when $P < .05$ for all tests.

Results

Hypoxia or HIF-1α Overexpression Induces MT4-MMP Expression

To identify the novel downstream targets of hypoxia in mediating cancer metastasis, cDNA microarray analysis was performed in the hypopharyngeal cancer cell line FADU under normoxic *versus* hypoxic conditions. The result showed a significant increase in *MT4-MMP* expression in FADU cells with hypoxia compared with cells in normoxic conditions (data not shown). Because MT4-MMP has been reported to be overexpressed in human cancers [22,23] and to promote

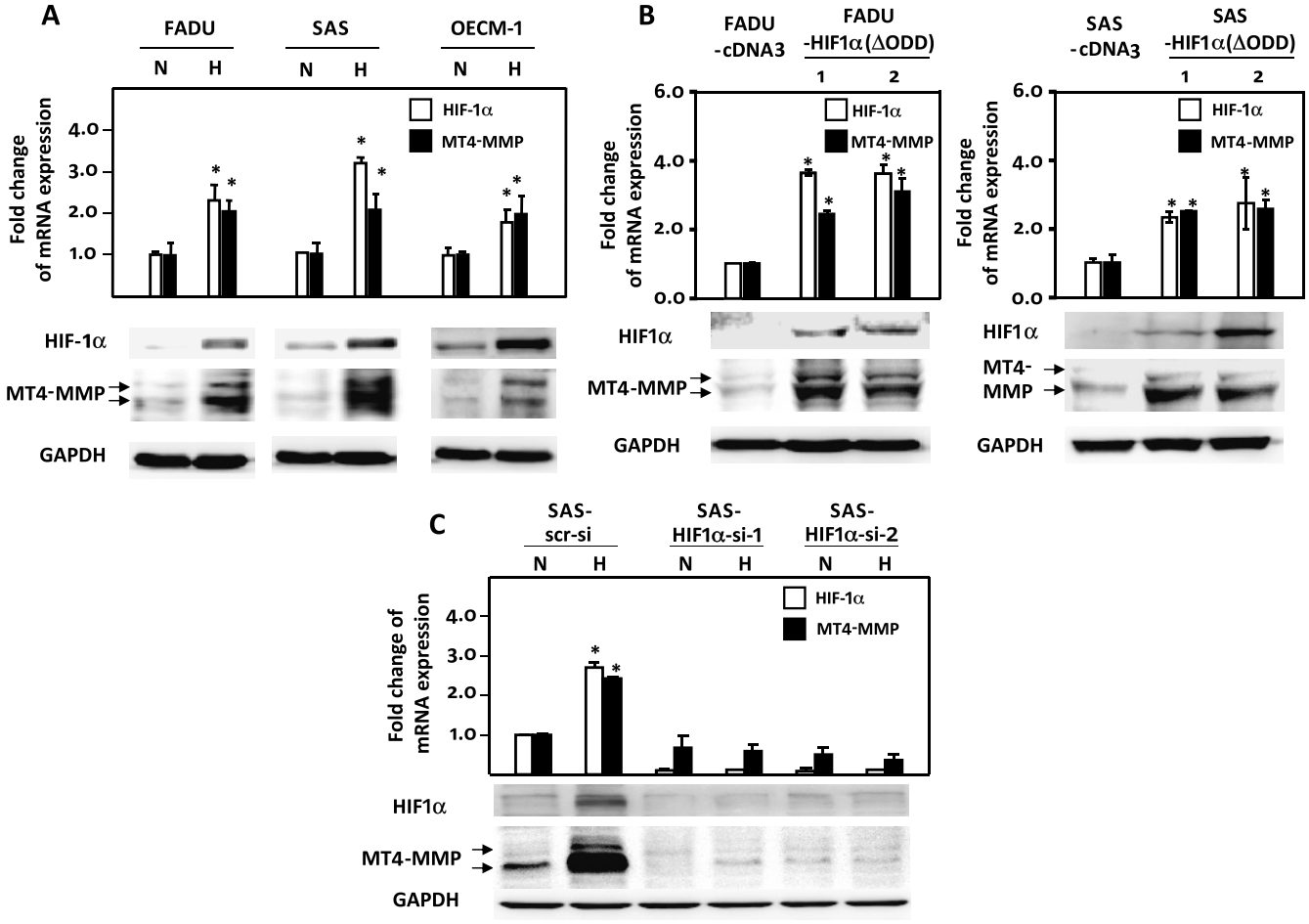

Figure 1. Hypoxia or constitutive expression of HIF-1α(ΔODD) upregulates *MT4-MMP* expression. (A) Upper: Fold change of mRNA levels of *HIF-1α* and *MT4-MMP* by real-time RT-PCR analysis in FADU, SAS, and OECM-1 cells under normoxia *versus* hypoxia. Lower: Western blot analysis of HIF-1α and MT4-MMP expression in FADU, SAS, and OECM-1 cells under normoxia *versus* hypoxia. (B) Upper: relative mRNA expression levels of *HIF-1α* and *MT4-MMP* in FADU-HIF1α(ΔODD) *versus* FADU-cDNA3 (left) and SAS-HIF1α(ΔODD) *versus* SAS-cDNA3. Lower: HIF-1α and MT4-MMP protein levels in FADU-HIF1α(ΔODD) *versus* FADU-cDNA3 (left) and SAS-HIF1α(ΔODD) *versus* SAS-cDNA3. (C) siRNA-mediated repression of endogenous HIF-1α abolishes the induction of MT4-MMP (mRNA and protein levels) in SAS cells under hypoxia. Transfection of the vector containing a scrambled sequence against human transcriptome (si-scr) was used as a control for siRNA experiments. The Western blot of MT4-MMP in all panels revealed two bands (*upper* indicates pro form; *lower*, active form) indicated by black arrows. GAPDH was used as a loading control for Western blot analysis. *N* indicates normoxia; *H*, hypoxia. The asterisk (*) indicated statistical significance ($P < .05$) between experimental and control clones.

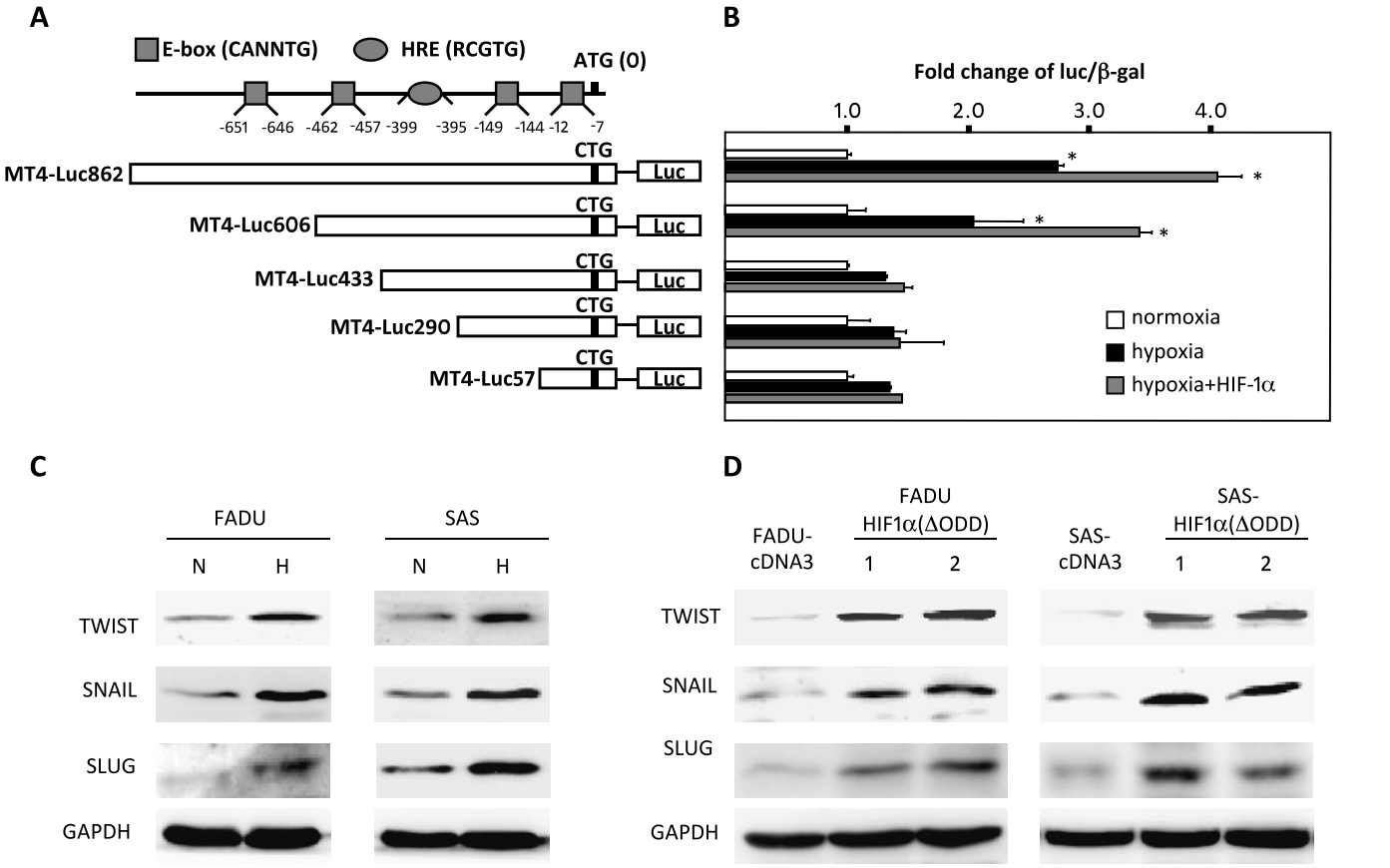

Figure 2. Mapping of the major regulatory region in *MT4-MMP* promoter responsible for HIF-1α–induced transcriptional activation, and hypoxia/HIF-1α upregulates the expression levels of SNAIL, TWIST, and SLUG. (A) Schematic representation of the promoter region of *MT4-MMP* and reporter constructs containing different lengths of *MT4-MMP* promoter. The E-boxes and hypoxia response element (HRE) are indicated. (B) Activation of MT4-Luc 862, MT4-Luc606, MT4-Luc433, MT4-Luc290, or MT4-Luc57 by hypoxia/HIF-1α overexpression. The luciferase activity/β-galactosidase of 293T cells cotransfected with MT4-Luc862/pcDNA3.1 was applied as the baseline control of other experiments (mean ± SD, $n = 3$; *$P < .05$ between experimental and control transfections). (C) Western blot analysis of TWIST, SNAIL, and SLUG expression in FADU and SAS cells under normoxia (N) *versus* hypoxia (H). (D) Western blot analysis of TWIST, SNAIL, and SLUG expression in FADU-HIF1α(ΔODD) *versus* FADU-cDNA3 (left) and SAS-HIF1α(ΔODD) *versus* SAS-cDNA3 (right).

metastasis [23,24], we speculated that MT4-MMP contributes to hypoxia-induced metastasis. Because of the paucity of published data on MT4-MMP in cancer cells, we firstly constructed the MT4-MMP expression vector pcDNA3–MT4-MMP and validated the expression efficiency of pcDNA3–MT4-MMP and the specificity of a commercialized anti–MT4-MMP antibody (M3684; Sigma-Aldrich, Corp, St. Louis, MO; see Table W2) by transient transfection of pcDNA3–MT4-MMP or an empty vector into 293T cells. For MT4-MMP protein expression, Western blot revealed two bands at the expected molecular weight (~64 kDa), with the upper one being the pro form and the lower one being the active form (Figure W1). This expression pattern was consistent with the previous report [23].

To test whether MT4-MMP was indeed upregulated under hypoxia in cancer cells, three HNSCC cell lines (hypopharyngeal cancer cell line FADU and oral cancer cell lines SAS and OECM-1) were subject to hypoxic stimulation. Quantitative real-time RT-PCR and Western blot analysis of HIF-1α and MT4-MMP were performed to evaluate differential HIF-1α/MT4-MMP expression under hypoxia *versus* normoxia. Up-regulation of the mRNA and protein levels of HIF-1α and MT4-MMP were demonstrated in all three cell lines under hypoxia (Figure 1*A*). These results indicate that hypoxia induces MT4-MMP expression in HNSCC cells.

Because the hypoxic response is mainly mediated by stabilization and activation of the hypoxia inducible factor-1 (HIF-1) transcriptional complex [30], we generated FADU and SAS clones, which constitutively expressed a HIF-1α mutant harboring a deletion of the oxygen degradation domain (ΔODD) that functions in a normoxic environment (FADU-HIF1α(ΔODD) and SAS-HIF1α(ΔODD)) [13,25]. When HIF-1α and MT4-MMP mRNA and protein levels were examined in FADU-HIF1α(ΔODD) *versus* FADU-cDNA3 and SAS-HIF1α(ΔODD) *versus* SAS-cDNA3, up-regulation of MT4-MMP mRNA and protein levels was demonstrated in the FADU-HIF1α(ΔODD) and SAS-HIF1α(ΔODD) clones (Figure 1*B*). To confirm that HIF-1α was mostly responsible for the induction of MT4-MMP by hypoxia, siRNA-mediated repression of HIF-1α was performed in SAS cells exposed to hypoxia. The results showed that repression of HIF-1α caused an almost complete repression of MT4-MMP mRNA and protein expression to levels present under normoxic conditions (Figure 1*C*). These findings suggested that a critical role for HIF-1α in the induction of MT4-MMP by hypoxia. As further confirmation, immunofluorescent staining demonstrated the membranous-cytoplasmic expression of MT4-MMP in SAS cells subjected to hypoxia but not in SAS cells under normoxia or SAS cells expressing an inactive HIF-1α mutant (HIF-1α-LCLL; see Figure W2*A*) [26]. Coexpression

HIF-1α and MT-MMP was also shown in human HNSCC primary tumor samples (Figure W2*B*). Collectively, these results indicate that hypoxia or HIF-1α overexpression induces MT4-MMP expression in HNSCC cells.

SLUG Is Responsible for Hypoxia or HIF-1α Overexpression–Induced MT4-MMP Expression

To elucidate the mechanism by which HIF-1α increases MT4-MMP expression, we generated the reporter construct MT4Luc862 containing proximal promoter region of MT4-MMP (Figure 2*A*). Transient transfection assay showed that activation of MT4Luc862 to three-folds after hypoxic incubation, and cotransfection with wild-type HIF-1α expression vector further increased the promoter activity to four-folds (Figure 2*B*). To map the major regulatory region of *MT4-MMP* promoter responsible for hypoxia/HIF-1α overexpression, different lengths of *MT4-MMP* promoter constructs were generated (MT4-Luc606, MT4-Luc433, MT4-Luc290, and MT4-Luc57; Figure 2*A*) and transactivation assays were performed. The results determined the major region responsible for HIF-1α–induced *MT4-MMP* transactivation: deletion of the E-box located in approximately –462 to –457 to ATG abolished the promoter activity under hypoxia/HIF-1α overexpression (Figure 2*B*). We therefore speculated that HIF-1α regulates *MT4-MMP* expression indirectly through an E-box–binding transcriptional factor. To find the E-box–binding transcriptional factor responsible of HIF-1α–induced *MT4-MMP* transcriptional activation, we firstly screened the expression levels of different E-box binding proteins in FADU and SAS cells subjected to hypoxia. The result demonstrated that SNAIL, TWIST, and SLUG were significantly

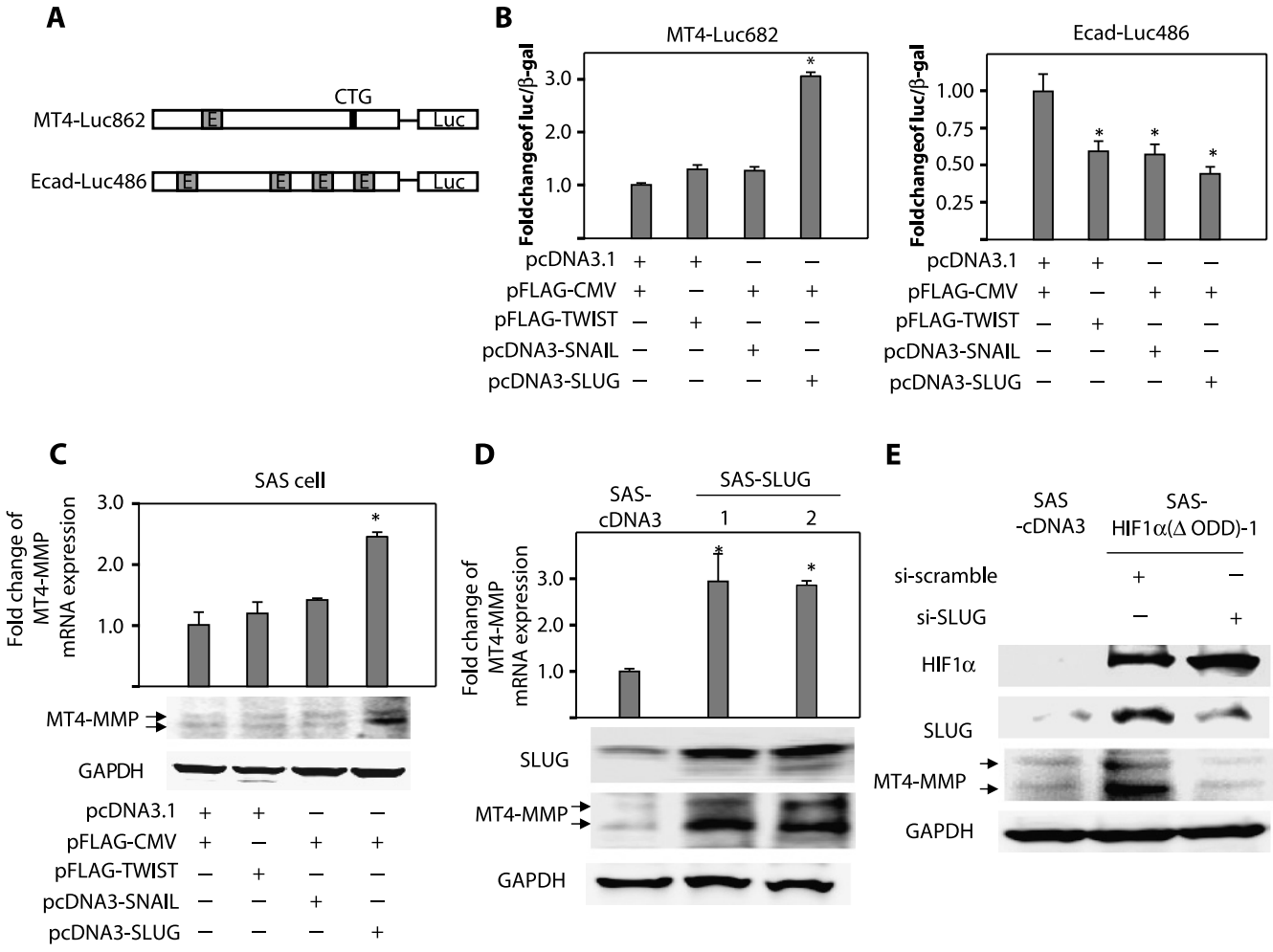

Figure 3. SLUG activates MT4-MMP expression and is critical for HIF-1α–mediated MT4-MMP induction. (A) Schematic representation of the reporter constructs containing proximal promoter of *MT4-MMP* (MT4-Luc862) or *E-cadherin* (Ecad-Luc486). (B) Left: Activation of MT4-Luc862 by overexpression of TWIST, SNAIL, or SLUG. Right: Repression of Ecad-Luc486 by overexpression of TWIST, SNAIL, or SLUG. The luciferase activity/β-galactosidase of 293T cells cotransfected with MT4-Luc862/pcDNA3.1/pFLAG-CMV (left) or Ecad-Luc486/pcDNA3.1/pFLAG-CMV (right) was applied as the baseline control of experiments (mean ± SD, $n = 3$; *$P < .05$ between experimental and control transfections). (C) Upper: Fold change of mRNA levels of *MT4-MMP* by real-time RT-PCR analysis in SAS cells overexpressing TWIST, SNAIL, or SLUG. Lower: Western blot analysis of MT4-MMP expression in SAS cells overexpressing TWIST, SNAIL, or SLUG. (D) Upper: Relative mRNA expression levels of *MT4-MMP* in SAS-SLUG *versus* SAS-cDNA3. Lower: Western blot analysis of SLUG and MT4-MMP expression in SAS-SLUG *versus* SAS-cDNA3. (E) siRNA-mediated repression of SLUG abolishes the HIF-1α–mediated induction of MT4-MMP expression in SAS cells. Transfection of the vector containing a scrambled sequence against human transcriptome (si-scr) was used as a control for siRNA experiments. The Western blot of MT4-MMP in (C), (D), and (E) revealed two bands (*upper* indicates pro form; *lower*, active form) indicated by black arrows. GAPDH was used as a loading control for Western blot analysis. *Statistical significance ($P < .05$) between experimental and control clones.

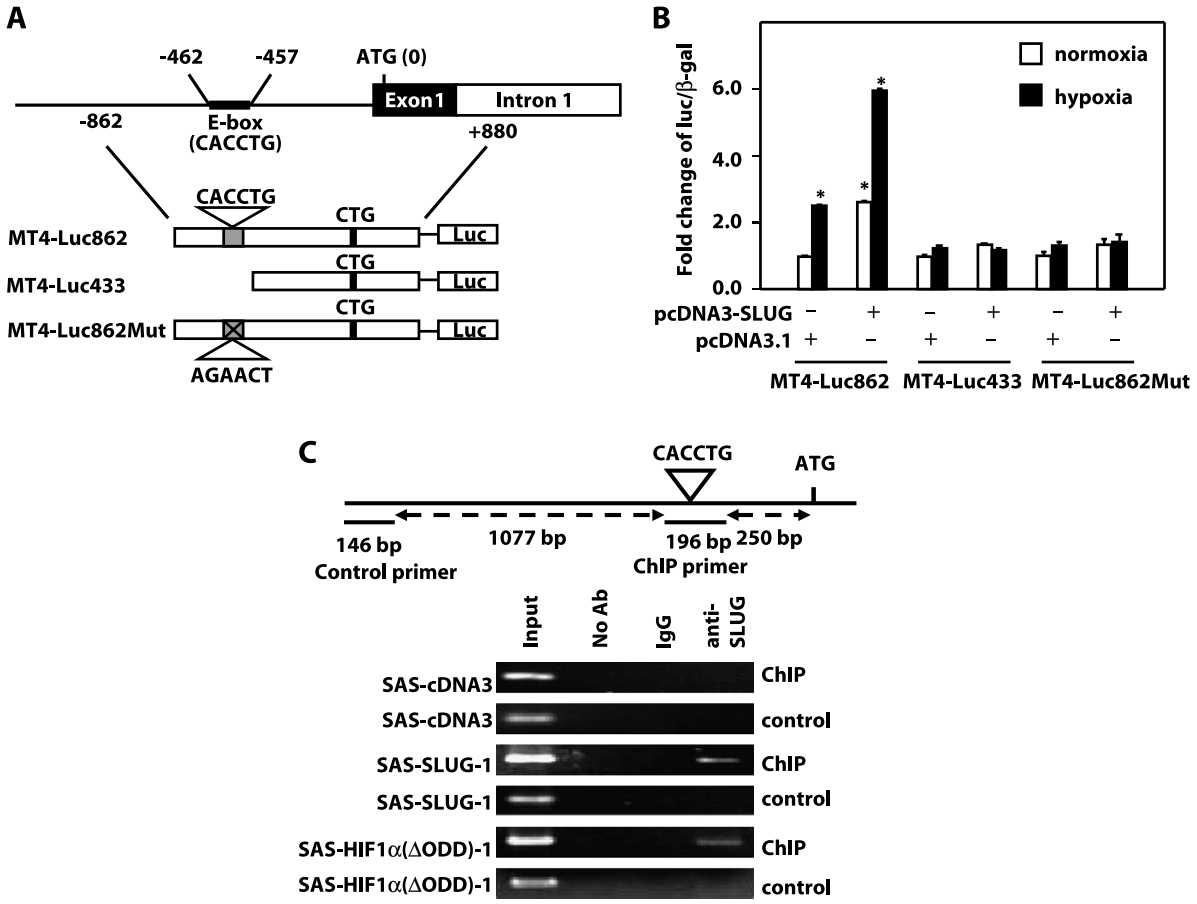

Figure 4. Direct regulation of *MT4-MMP* by SLUG. (A) Schematic representation of the genomic organization of the promoter region of *MT4-MMP* and reporter constructs used in transient transfection assays. The constructs were wild-type (MT4-Luc862), E-Box–deleted (MT4-Luc433), or E-box–mutated (MT4-Luc862Mut). (B) Transcriptional activation of MT4-Luc862, but not MT4-Luc433 and MT4-Luc862Mut by SLUG, hypoxia or SLUG + hypoxia. The luciferase activity/β-galactosidase of 293T cells cotransfected with MT4-Luc862/pcDNA3.1 was applied as the baseline control of other experiments (mean ± SD, $n = 3$; $^*P < .05$ between experimental and control transfections). (C) ChIP analysis of SAS-SLUG, SAS-HIF1α(ΔODD) *versus* SAS-cDNA3. Chromatin was incubated without antibody, with an IgG, or with an anti-SLUG antibody. The 196-bp fragment contains the Slug binding sequence, whereas the 146-bp fragment does not contain any Slug binding sequence. Schematic representation of the design of ChIP and control primers was shown in the upper panel. Input: 2% of total input lysate.

upregulated under hypoxia in both cell lines (Figure 2*C*), and a consistent result was shown in FADU or SAS cells overexpressing HIF-1α (Figure 2*D*). To determine the major factor contributing to HIF-1α–induced *MT4-MMP* up-regulation, transient transfection assay was performed in 293T cells cotransfected with the MT4-Luc862 and different expression vectors (pcDNA3-SNAIL, pcDNA3-SLUG, or pFLAG-TWIST) or control vectors (pcDNA3.1 or pFLAG-CMV). We also generated a reporter construct containing the proximal promoter of *E-cadherin* (Ecad-Luc486) to confirm the suppressive effect of SNAIL/TWIST/SLUG to *E-cadherin* promoter as a control of the experiment (Figure 3*A*). The result demonstrated that SNAIL, SLUG, and TWIST all harbored the inhibitory effect to *E-cadherin* promoter (Figure 3*B*, *right panel*); however, activation of *MT4-MMP* promoter was only shown in SLUG-overexpressing cells (Figure 3*B*, *left panel*). This result indicates that SLUG is the major factor contributing to *MT4-MMP* transactivation. To confirm this finding, overexpression of SNAIL, SLUG, or TWIST was performed in SAS cells, and the protein and mRNA levels of MT4-MMP were evaluated. Increased MT4-MMP mRNA and protein expression was shown in SAS cells overexpressing SLUG but not SNAIL or TWIST (Figure 3*C*). To further validate this result, we generated SAS clones with stable SLUG expression (SAS-SLUG clones; Figure 3*D*). An increase in MT4-MMP mRNA and protein levels was demonstrated in the SAS-SLUG clones compared with the control cells (Figure 3*D*). To demonstrate the critical role of SLUG in HIF-1α–induced MT4-MMP expression, siRNA-mediated repression of *SLUG* was performed in SAS-HIF1α(ΔODD) cells. As predicted, MT4-MMP expression decreased after siRNA-mediated repression of *SLUG* (Figure 3*E*). Collectively, these results suggest that SLUG is the major factor responsible for hypoxia/HIF-1α–induced MT4-MMP expression.

Direct Regulation of MT4-MMP Expression by SLUG

To determine whether *MT4-MMP* is directly regulated by SLUG, a putative SLUG binding site (the E-box sequence CACCTG; approximately –457 to –462 bp upstream from ATG) was identified in the proximal promoter of the *MT4-MMP* gene (Figure 4*A*). Transient transfection assays showed a two- to three-fold increase in *MT4-MMP* promoter activity after cotransfection with a SLUG expression vector or with hypoxic incubation. Interestingly, hypoxia augmented SLUG-induced *MT4-MMP* promoter activation by six-fold. Deletion or site-directed mutagenesis of the SLUG binding site eliminated promoter activation mediated by SLUG or hypoxia (Figure 4*B*). To

confirm the *in vivo* binding of SLUG to the E-box in the *MT4-MMP* promoter in HNSCC cells overexpressing HIF-1α or SLUG, ChIP assays were performed in SAS-SLUG and SAS-HIF1α(ΔODD) *versus* SAS-cDNA3 cell lines. The results showed that the PCR-amplified fragments in the *MT4-MMP* promoter region containing the E-box site (196 bp) could be retrieved from the immunoprecipitates by an anti-SLUG antibody in both the SAS-SLUG and SAS-HIF1α(ΔODD) samples but not in the SAS-cDNA3 sample (Figure 4*C*). These results demonstrate that SLUG activates *MT4-MMP* transcription through direct interaction with the E-box located in the proximal promoter of the *MT4-MMP* gene.

MT4-MMP Contributes to HIF-1α– or SLUG-induced In Vitro *Invasiveness and Pulmonary Colonization in Tail Vein Assay*

To test whether MT4-MMP is critical for HIF-1α– or SLUG-induced *in vitro* migration/invasion and *in vivo* settlement of tumor cells in the lungs, *in vitro* migration/invasion assays and *in vivo* tail vein assays were performed using the SAS-cDNA3 clone, SAS-HIF1α(ΔODD) clones transfected with siRNA against *SLUG* or *MT4-MMP*, and SAS-SLUG clones transfected with siRNA against *MT4-MMP*. For the migration assays, overexpression of HIF-1α and SLUG increased the migratory ability of SAS cells by approximately three- to four-fold. Knockdown of SLUG in SAS-HIF1α(ΔODD) clones partially suppressed migration. However, knockdown of MT4-MMP did not influence cell migratory ability in either SAS-HIF1α(ΔODD) or SAS-SLUG cell lines (Figure 5*A*).

A different scenario was observed in the invasion assays. Overexpression of HIF-1α and SLUG increased cell invasiveness by approximately four- to five-fold, and knockdown of SLUG in SAS-HIF1α(ΔODD) clones partially abolished cell invasiveness. Suppression of MT4-MMP also inhibited the invasiveness in both SAS-HIF1α(ΔODD) and SAS-SLUG clones (Figure 5*B*). A similar result was demonstrated in the tail vein assay. Repression of SLUG in SAS-HIF1α(ΔODD) clones

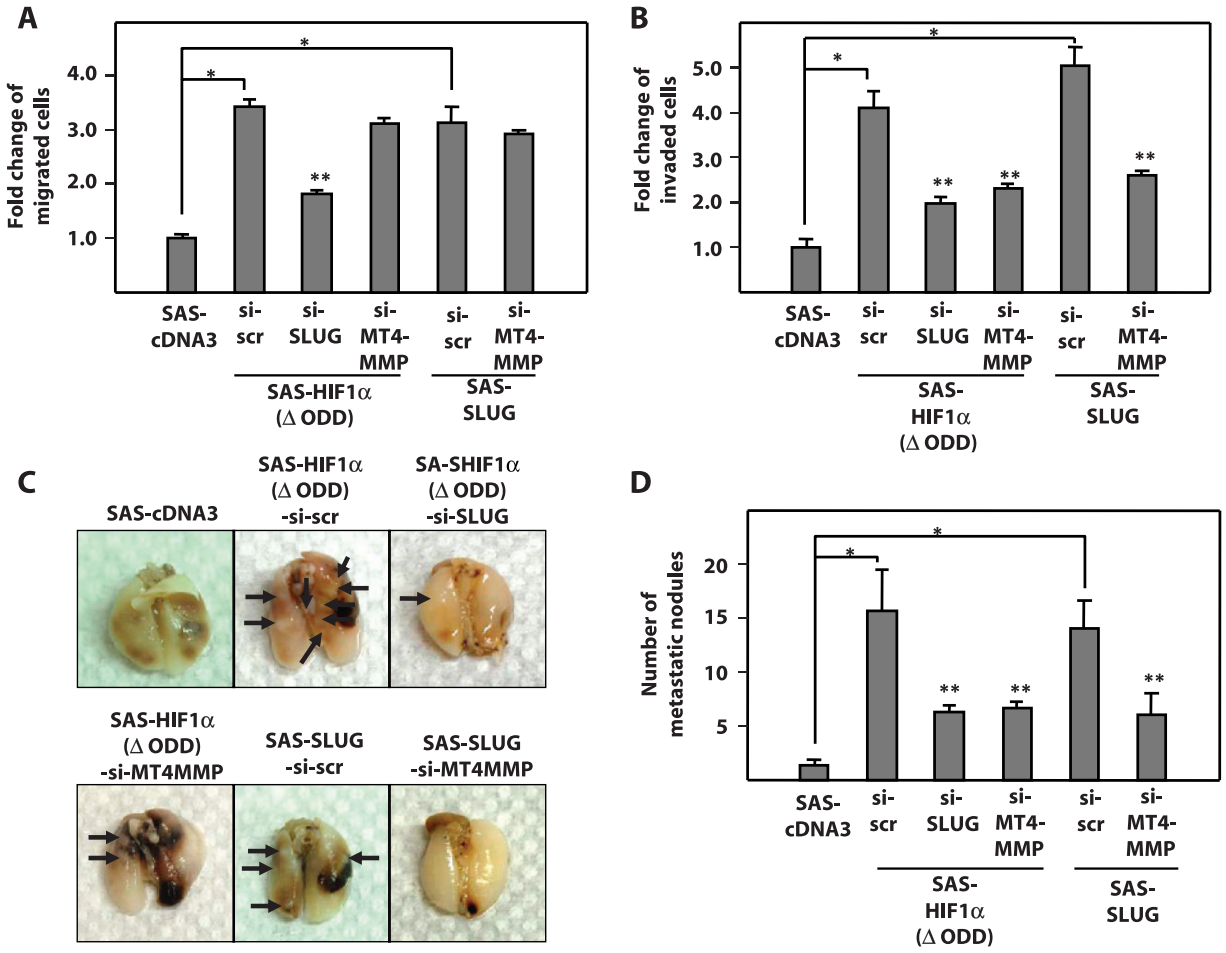

Figure 5. MT4-MMP is critical in HIF-1α or SLUG mediated invasion and pulmonary colonization of tumor cells. (A) Fold change of migratory ability of SAS-HIF1α(ΔODD) receiving siRNA against SLUG or MT4-MMP, and SAS-SLUG receiving siRNA-mediated MT4-MMP repression. (B) Fold change of invasiveness of SAS-HIF1α(ΔODD) receiving siRNA against SLUG or MT4-MMP, and SAS-SLUG receiving siRNA-mediated MT4-MMP repression. (C) Representative pictures of metastatic pulmonary nodules (indicated by black arrows) in mice receiving SAS-cDNA3, SAS-HIF1α(ΔODD)-si-scr, SAS-HIF1α(ΔODD)-si-SLUG, SAS-HIF1α(ΔODD)-si–MT4-MMP, SAS-SLUG-si-scr, and SAS-SLUG-si–MT4-MMP injections. (D) Fold change of pulmonary tumor nodules of SAS-HIF1α(ΔODD) receiving siRNA against SLUG or MT4-MMP, and SAS-SLUG receiving siRNA-mediated MT4-MMP repression. The migration/invasion/metastasis of SAS-cDNA3 clone was used as the baseline control of all experiments, whereas transfection of the vector containing a scrambled sequence (si-scr) was used as a control of siRNA experiments. *Statistical significance ($P < .05$) between the baseline control clone (SAS-cDNA3) and SAS-HIF1α(ΔODD)-si-scr/SAS-SLUG-si-scr; **statistical significance ($P < .05$) between siRNA experimental clones (si-SLUG or si–MT4-MMP) and si-scr clones.

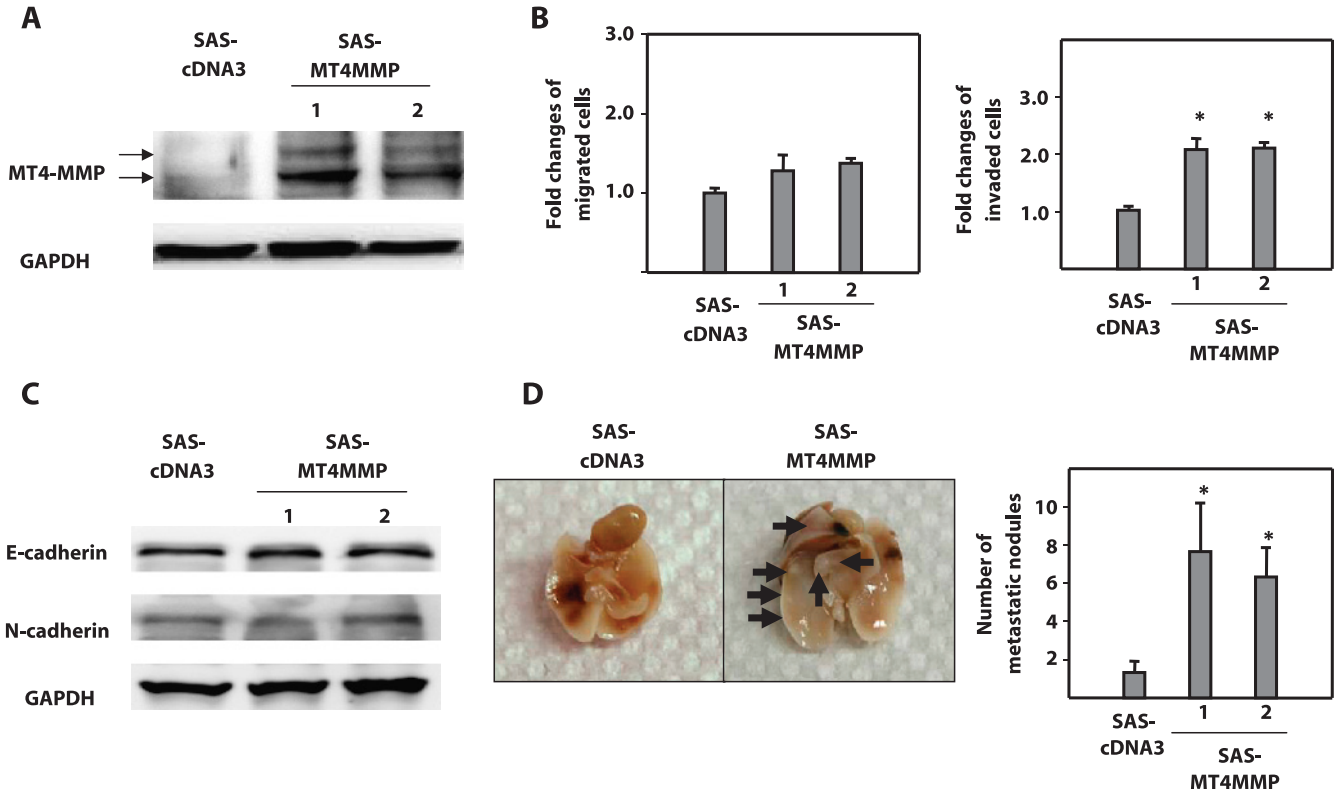

Figure 6. MT4-MMP contributes to invasiveness and pulmonary colonization of tumor cells through an EMT-independent mechanism. (A) Western blot analysis MT4-MMP in SAS–MT4-MMP *versus* SAS-cDNA3. GAPDH was used as a loading control for Western blot analysis. The Western blot of MT4-MMP revealed two bands (*upper* indicates pro form; *lower*, active form) indicated by black arrows. (B) Fold change of migratory ability (left) and invasiveness (right) of SAS–MT4-MMP *versus* SAS-cDNA3. (C) Western blot analysis the epithelial (E-cadherin) and mesenchymal (N-cadherin) markers in SAS–MT4-MMP *versus* SAS-cDNA3. (D) Left: Representative pictures of metastatic pulmonary nodules (indicated by black arrows) in mice receiving SAS–MT4-MMP *versus* SAS-cDNA3 injections. Right: Number of metastatic nodules counted in mice receiving SAS–MT4-MMP *versus* SAS-cDNA3 injections. *Statistical significance ($P < .05$) between experimental clones and baseline control clone (SAS-cDNA3).

decreased the capacity of tumor growth in the lung in these cells. Inhibition of MT4-MMP expression also decreased pulmonary colonization of both SAS-HIF1α(ΔODD) and SAS-SLUG clones (Figure 5, *C* and *D*). These results showed that MT4-MMP participates in HIF-1α– or SLUG-induced invasiveness and pulmonary colonization of cancer cells without any substantial effects on cell migratory ability.

MT4-MMP Promotes In Vitro *Invasiveness and* In Vivo *Colonization and Growth of Tumor Cells in the Lungs, Which Is Independent of EMT*

To investigate whether overexpression of MT4-MMP alone could induce metastasis, SAS clones that stably expressed MT4-MMP (SAS–MT4-MMP) were generated (Figure 6*A*). When the ability of MT4-MMP to induce cell migration and invasion was tested, the results showed that overexpression of MT4-MMP promoted SAS cell invasiveness but not cell migration (Figure 6*B*). Because the induction of EMT is critical for cancer metastasis, we evaluated changes in EMT marker expression in SAS–MT4-MMP and SAS-cDNA3 cells. The results showed that the expression levels of the epithelial marker E-cadherin and mesenchymal marker N-cadherin were not different in the experimental and control clones (Figure 6*C*). However, MT4-MMP significantly promoted the settlement and growth of tumor cells in the lung in the tail vein metastasis assay (Figure 6*D*). These results suggested that MT4-MMP may contribute to *in vitro* invasiveness and *in vivo* colonization and growth of tumor cells in the lungs, which is independent of EMT.

To test the influence of MT4-MMP on MMP and angiogenic factor expression profiles, the major cytokine families involved in cancer cell invasiveness and metastasis, antibody arrays, including MMPs arrays and angiogenic factors arrays, were screened using SAS–MT4-MMP and SAS-cDNA3 cells. The results indicated that MT4-MMP indeed influenced the expression profiles of MMPs and angiogenic factors, with the decreased expression of MMP-8, tissue inhibitor of metalloproteinase-4 (TIMP-4; Figure W3, *A* and *B*), TIMP-2 (Figure W3, *A–D*), and increased expression of basic fibroblastic growth factor (Figure W3, *C* and *D*). Collectively, our results showed that overexpression of MT4-MMP in cancer cells promoted invasiveness and settlement of tumor cells in the lung through an EMT-independent mechanism, possibly involving modulation of certain MMP family proteins and angiogenic factors.

Coexpression of HIF-1α and MT4-MMP Is a Prognostic Marker of Human HNSCC

To investigate the clinical significance of MT4-MMP overexpression in HNSCC and its relationship to HIF-1α expression, IHC analysis of HIF-1α and MT4-MMP expression was performed using 68 human HNSCC archived samples (Table 1). The specificity of

the antibodies used in IHC experiments was validated by ICC assay (Figure W4). The IHC results of two representative cases (case A, coexpression of both markers; case B, negative for both markers) are presented in Figure 7*A*. Overexpression of HIF-1α or MT4-MMP detected by IHC was confirmed in 41.2% and 54.4% of cases, respectively (Table 1). Overexpression of HIF-1α was also associated with a worse prognosis of HNSCC cases (P = .006; Table 1), and there was also a trend toward a worse outcome in patients overexpressing MT4-MMP (P = .081; Table 1). Overexpression of HIF-1α was closely associated with increased MT4-MMP expression (P = .018; Table 2). To demonstrate the prognostic significance of the expression pattern of HIF-1α and/or MT4-MMP in HNSCCs, we divided the patients into four protein expression groups, namely HIF-1α(–)/MT4-MMP(–), HIF-1α(+)/MT4-MMP(–), HIF-1α(–)/MT4-MMP(+), and HIF-1α(+)/MT4-MMP(+), and performed a Kaplan-Meier survival analysis. When compared with other groups, patients with the expression pattern of HIF-1α(+)/MT4-MMP(+) had a worse

Table 2. Correlation of the IHC Expression of HIF-1α and MT4-MMP in Primary Tumor Samples of 68 HNSCC Cases.

		MT4-MMP		*P*
		Negative	Positive	
HIF-1α	Negative	23	17	.018
	Positive	8	20	

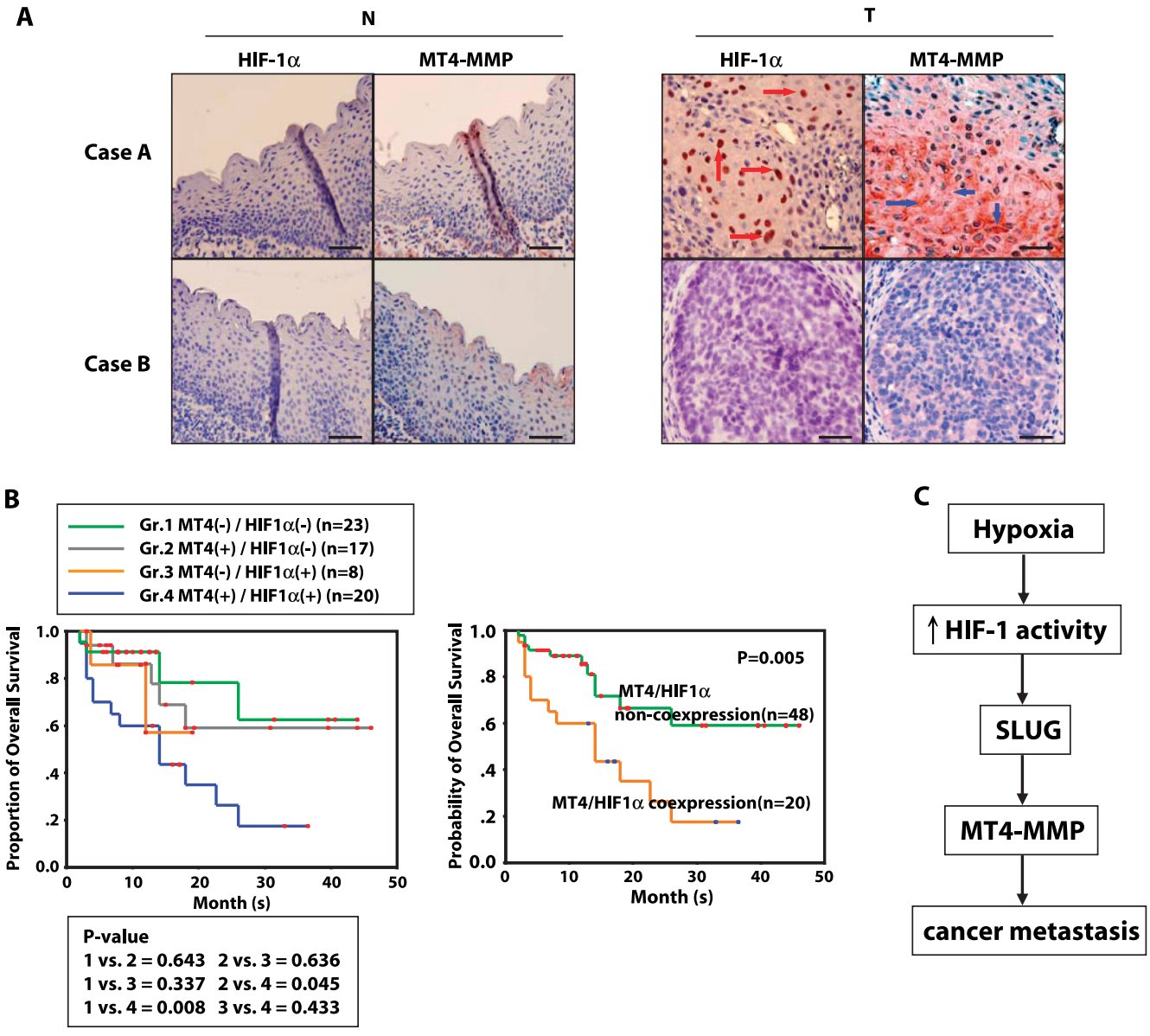

Figure 7. Coexpression of HIF-1α and MT4-MMP in HNSCC cases indicates a worse survival, and a proposed model of hypoxia induced metastasis through activation of MT4-MMP. (A) IHC staining of HIF-1α and MT4-MMP in two representative HNSCC cases with coexpression of HIF-1α/MT4-MMP (upper panel, cases A) and negative for both markers (lower panel, case B). *N* indicates normal epithelium; *T*, tumor tissues. The red arrows indicate the nucleus expression of HIF-1α, whereas the blue arrows indicate the membranocytoplasmic expression of MT4-MMP. Scale bars, 200 μm. (B) Left: Comparison of the overall survival period of patients categorized by HIF-1α/MT4-MMP IHC result. Right: Survival difference in HNSCC cases with or without HIF-1α/MT4-MMP coexpression. (C) A proposed model of hypoxia induced metastasis through MT4-MMP.

prognosis (Figure 7*B*, *left panel*). We therefore divided cases into HIF-1α/MT4-MMP coexpression *versus* non-coexpression. The coexpression cases had a significantly worse survival than did non-coexpression cases ($P = .005$; Figure 7*B*, *right panel*). These results support our observations from cell lines that activation of MT4-MMP by HIF-1α/SLUG contributes to HNSCC metastasis.

Discussion

Increasing evidence indicates that tumor hypoxia has a critical role in the promotion of metastasis through the induction of angiogenesis and EMT. However, data addressing hypoxia/HIF-1α modulation of tumor cell invasive proteolytic enzyme expression are relatively scarce, with the exceptions of the activation of cathepsin D, MMP-2, urokinase plasminogen activator receptor, plasminogen activator inhibitor-1, and protease activator receptor-1 by HIF-1α [14,15,31,32]. Here, we provide evidence that activation of MT4-MMP by SLUG contributes to hypoxia/HIF-1α–mediated cancer invasiveness and metastasis. In support of this possibility, we have shown that hypoxia/HIF-1α induces MT4-MMP expression through the activation of SLUG, *MT4-MMP* is directly regulated by SLUG through binding to its proximal promoter, MT4-MMP is critical for HIF-1α– or SLUG-induced invasiveness/settlement and growth of tumor cells in the lung, MT4-MMP promotes invasiveness and pulmonary colonization of cancer cells through modulation of the invasive proteome and angiogenesis in an EMT-independent mechanism, and tumor coexpression of HIF-1α and MT4-MMP indicates a worse prognosis in patients head and neck cancer. These results demonstrate a novel signaling pathway in hypoxia-mediated metastasis and highlight the critical role of MT4-MMP in hypoxic tumors.

As one of the major family of proteins involved in cancer metastasis, correlations between MMPs and EMT have been well documented. Different MMPs have been shown to be regulated by regulators of EMT. For example, MMP-2 and MMP-9 are regulated by SNAIL [33,34]. In the present report, we demonstrate that SLUG, a zinc-finger transcriptional factor that induces EMT through suppression of E-cadherin expression [35,36], regulates MT4-MMP expression, further supporting the correlation between EMT and MMPs. Among the known MMPs, only MMP-3 has been shown to induce EMT through Rac1b activity and increased concentrations of reactive oxygen species [37]. In contrast to MMP-3, MT4-MMP was unable to induce EMT in cancer cells. This result suggests that MT4-MMP is located downstream of the hypoxia/EMT signal pathway and that it mediates cancer metastasis.

Although MT4-MMP was shown to induce the *in vivo* metastasis of breast cancer cells [23], the effect of MT4-MMP on the migratory ability/invasiveness of cancer cells remains to be unequivocally demonstrated. Chabottaux et al. [23] reported that overexpression of MT4-MMP did not affect the *in vitro* invasiveness of the breast cancer cell line MDA-MB231 in a Boyden chamber assay. However, Rizki et al. [38] suggested that MT4-MMP is functionally significant in the acquisition of invasiveness. Using a similar assay, he demonstrated that knockdown of MT4-MMP suppressed the invasiveness of HMT-3522 breast tumor cells. In our study, we have shown that overexpression of MT4-MMP had no effect on the migratory ability of cancer cells but contributed significantly to both *in vitro* invasiveness and *in vivo* settlement of tumor cells in the lung in the tail vein assay. These results were consistent with the outcome of siRNA experiments, in which suppression of MT4-MMP in HNSCC cells overexpressing HIF-1α or SLUG partially reduced *in vitro* cellular invasiveness and *in vivo* pulmonary colonization of tumor cells without affecting cell migratory ability. Because EMT is the major mechanism responsible for cancer cell migration [39], we speculated that MT4-MMP may contribute to *in vitro* invasiveness and *in vivo* pulmonary colonization of tumor cells through an EMT-independent mechanism. Cytokine array experiments demonstrated MT4-MMP modulates the expression profile of MMP family proteins and angiogenic factors, including decreased expression of MMP-8, TIMP-2, and TIMP-4 and increased expression of basic fibroblast growth factor. In this regard, repression of MMP-8, which functions as a tumor suppressor and is known as an "antitarget" for cancer therapy [40,41], by MT4-MMP leads to the promotion of tumor metastasis and has a negative impact on patient outcome. According to the above findings, we suggest that MT4-MMP may contribute to invasiveness through the modulation of the invasive proteome of tumor cells. Considering the effect of MT4-MMP in the tail vein assay, we suggest that MT4-MMP facilitates settlement and growth of tumor cells in the lung by a so-far unknown mechanism because the tail vein injection of tumor cells into NOD-SCID mice cannot totally reflect the metastatic ability of cancer cells. The underlying cause of increased pulmonary colonization in MT4-MMP overexpressing cancer cells may attribute to the modulation of invasive proteome and angiogenic ability.

In conclusion, this report establishes a new, stepwise signaling pathway from hypoxia/HIF-1 to SLUG to MT4-MMP and demonstrates the critical role of MT4-MMP in hypoxia-induced cancer cell metastasis. A new proposed model for this pathway is outlined in Figure 7*C*. These results should significantly impact future cancer therapeutic interventions and avenues for the prevention of hypoxic tumor metastasis.

Acknowledgments

The authors thank L.E. Huang (University of Utah) for the generous gifts of the plasmids pHA-HIF1α, pHA-HIF1α(ΔODD), and pHA-HIF1α(LCLL) and T.Y. Chou and W.Y. Li of the Department of Pathology, Taipei Veterans General Hospital, for providing expert opinions on the pathology readings and IHC analyses.

References

[1] Harris AL (2002). Hypoxia—a key regulatory factor in tumor growth. *Nat Rev Cancer* **2**, 38–47.

[2] Maxwell PH (2005). The HIF pathway in cancer. *Semin Cell Dev Biol* **16**, 523–530.

[3] Bertout JA, Patel SA, and Simon MC (2008). The impact of O_2 availability on human cancer. *Nat Rev Cancer* **8**, 967–975.

[4] Yang MH and Wu KJ (2008). TWIST activation by hypoxia inducible factor-1 (HIF-1): implications in metastasis and development. *Cell Cycle* **7**, 2090–2096.

[5] Mikhaylova M, Mori N, Wildes FB, Walczak P, Gimi B, and Bhujwalla ZM (2008). Hypoxia increases breast cancer cell–induced lymphatic endothelial cell migration. *Neoplasia* **10**, 380–388.

[6] Forsythe JA, Jiang BH, Iyer NV, Agani F, Leung SW, Koos RD, and Semenza GL (1996). Activation of vascular endothelial growth factor gene transcription by hypoxia-inducible factor 1. *Mol Cell Biol* **16**, 4604–4613.

[7] Folkman J (2002). Role of angiogenesis in tumor growth and metastasis. *Semin Oncol* **29** (6 Suppl 16), 15–18.

[8] Imai T, Horiuchi A, Wang C, Oka K, Ohira S, Nikaido T, and Konishi I (2003). Hypoxia attenuates the expression of E-cadherin via up-regulation of SNAIL in ovarian carcinoma cells. *Am J Pathol* **163**, 1437–1447.

[9] Kurrey NK, K A, and Bapat SA (2005). Snail and Slug are major determinants of ovarian cancer invasiveness at the transcription level. *Gynecol Oncol* **97**, 155–165.

[10] Krishnamachary B, Zagzag D, Nagasawa H, Rainey K, Okuyama H, Baek JH, and Semenza GL (2006). Hypoxia-inducible factor-1–dependent repression of E-cadherin in von Hippel-Lindau tumor suppressor-null renal carcinoma mediated by TCF3, ZFHX1A, and ZFHX1B. *Cancer Res* **66**, 2725–2731.

[11] Evans AJ, Russell RC, Roche O, Burry TN, Fish JE, Chow VW, Kim WY, Saravanan A, Maynard MA, Gervais ML, et al. (2007). VHL promotes E2 box-dependent E-cadherin transcription by HIF-mediated regulation of SIP1 and Snail. *Mol Cell Biol* **27**, 157–169.

[12] Peinado H and Cano A (2008). A hypoxic twist in metastasis. *Nat Cell Biol* **10**, 253–254.

[13] Yang MH, Wu MZ, Chiou SH, Chen PM, Chang SY, Liu CJ, Teng SC, and Wu KJ (2008). Direct regulation of TWIST by HIF-1α promotes metastasis. *Nat Cell Biol* **10**, 295–305.

[14] Krishnamachary B, Berg-Dixon S, Kelly B, Agani F, Feldser D, Ferreira G, Iyer N, LaRusch J, Pak B, Taghavi P, et al. (2003). Regulation of colon carcinoma cell invasion by hypoxia-inducible factor 1. *Cancer Res* **63**, 1138–1143.

[15] Büchler P, Reber HA, Tomlinson JS, Hankinson O, Kallifatidis G, Friess H, Herr I, and Hines OJ (2009). Transcriptional regulation of urokinase-type plasminogen activator receptor by hypoxia-inducible factor 1 is crucial for invasion of pancreatic and liver cancer. *Neoplasia* **11**, 196–206.

[16] Streuli C (1999). Extracellular matrix remodelling and cellular differentiation. *Curr Opin Cell Biol* **11**, 634–640.

[17] Stamenkovic I (2000). Matrix metalloproteinases in tumor invasion and metastasis. *Semin Cancer Biol* **10**, 415–433.

[18] Egeblad M and Werb Z (2002). New functions for the matrix metalloproteinases in cancer progression. *Nat Rev Cancer* **2**, 161–174.

[19] Deryugina EI and Quigley JP (2006). Matrix metalloproteinases and tumor metastasis. *Cancer Metast Rev* **25**, 9–34.

[20] Sohail A, Sun Q, Zhao H, Bernardo MM, Cho JA, and Fridman R (2008). MT4-(MMP17) and MT6-MMP (MMP25), a unique set of membrane-anchored matrix metalloproteinases: properties and expression in cancer. *Cancer Metast Rev* **27**, 289–302.

[21] English WR, Puente XS, Freije JM, Knauper V, Amour A, Merryweather A, Lopez-Otin C, and Murphy G (2000). Membrane type 4 matrix metalloproteinase (MMP17) has tumor necrosis factor-alpha convertase activity but does not activate pro-MMP2. *J Biol Chem* **275**, 14046–14055.

[22] Puente XS, Pendas AM, Llano E, Velasco G, and Lopez-Otin C (1996). Molecular cloning of a novel membrane-type matrix metalloproteinase from a human breast carcinoma. *Cancer Res* **56**, 944–949.

[23] Chabottaux V, Sounni NE, Pennington CJ, English WR, van den Brûle F, Blacher S, Gilles C, Munaut C, Maquoi E, Lopez-Otin C, et al. (2006). Membrane-type 4 matrix metalloproteinase promotes breast cancer growth and metastases. *Cancer Res* **66**, 5165–5172.

[24] Chabottaux V, Ricaud S, Host L, Blacher S, Paye A, Thiry M, Garofalakis A, Pestourie C, Gombert K, Bruyere F, et al. (2009). Membrane-type 4 matrix metalloproteinase (MT4-MMP) induces lung metastasis by alteration of primary breast tumor vascular architecture. *J Cell Mol Med* [Epub ahead of print May 1].

[25] Huang LE, Gu J, Schau M, and Bunn HF (1998). Regulation of hypoxia-inducible factor 1α is mediated by an O_2-dependent degradation domain via the ubiquitin-proteasome pathway. *Proc Natl Acad Sci USA* **95**, 7987–7992.

[26] Koshiji M, Kageyama Y, Pete EA, Horikawa I, Barrett JC, and Huang LE (2004). HIF-1α induces cell cycle arrest by functionally counteracting Myc. *EMBO J* **23**, 1949–1956.

[27] Yang L, Xie S, Jamaluddin MS, Altuwaijri S, Ni J, and Kim E (2005). Induction of androgen receptor expression by phosphatidylinositol 3-kinase/Akt downstream substrate, FOXO3a, and their roles in apoptosis of LNCaP prostate cancer cells. *J Biol Chem* **280**, 33558–33565.

[28] Yang MH, Chiang WC, Chou TY, Chang SY, Chen PM, Teng SC, and Wu KJ (2006). Increased NBS1 expression is a marker of aggressive head and neck cancer and overexpression of NBS1 contributes to transformation. *Clin Cancer Res* **12**, 507–515.

[29] Yang MH, Chang SY, Chiou SH, Liu CJ, Chi CW, Chen PM, Teng SC, and Wu KJ (2007). Overexpression of NBS1 induces epithelial-mesenchymal transition and co-expression of NBS1 and Snail predicts metastasis of head and neck cancer. *Oncogene* **26**, 1459–1467.

[30] Semenza GL (2002). Targeting HIF-1 for cancer therapy. *Nat Rev Cancer* **2**, 38–47.

[31] Lin MT, Kuo IH, Chang CC, Chu CY, Chen HY, Lin BR, Sureshbabu M, Shih HJ, and Kuo ML (2008). Involvement of hypoxia-inducing factor-1α–dependent plasminogen activator inhibitor-1 up-regulation in Cyr61/CCN1–induced gastric cancer cell invasion. *J Biol Chem* **283**, 15807–15815.

[32] Naldini A, Filippi I, Ardinghi C, Silini A, Giavazzi R, and Carraro F (2009). Identification of a functional role for the protease-activated receptor-1 in hypoxic breast cancer cells. *Eur J Cancer* **45**, 454–460.

[33] Yokoyama K, Kamata N, Fujimoto R, Tsutsumi S, Tomonari M, Taki M, Hosokawa H, and Nagayama M (2003). Increased invasion and matrix metalloproteinase-2 expression by Snail-induced mesenchymal transition in squamous cell carcinomas. *Int J Oncol* **22**, 891–898.

[34] Olmeda D, Jordá M, Peinado H, Fabra A, and Cano A (2007). Snail silencing effectively suppresses tumour growth and invasiveness. *Oncogene* **26**, 1862–1874.

[35] Hajra KM, Chen DY, and Fearon ER (2002). The SLUG zinc-finger protein represses E-cadherin in breast cancer. *Cancer Res* **62**, 1613–1618.

[36] Bolós V, Peinado H, Pérez-Moreno MA, Fraga MF, Esteller M, and Cano A (2003). The transcription factor Slug represses E-cadherin expression and induces epithelial to mesenchymal transitions: a comparison with Snail and E47 repressors. *J Cell Sci* **116** (Pt 3), 499–511.

[37] Radisky DC, Levy DD, Littlepage LE, Liu H, Nelson CM, Fata JE, Leake D, Godden EL, Albertson DG, Nieto MA, et al. (2005). Rac1b and reactive oxygen species mediate MMP-3–induced EMT and genomic instability. *Nature* **436**, 123–127.

[38] Rizki A, Weaver VM, Lee SY, Rozenberg GI, Chin K, Myers CA, Bascom JL, Mott JD, Semeiks JR, Grate LR, et al. (2008). A human breast cell model of preinvasive to invasive transition. *Cancer Res* **68**, 1378–1387.

[39] Thiery JP (2002). Epithelial-mesenchymal transitions in tumour progression. *Nat Rev Cancer* **2**, 442–454.

[40] Balbín M, Fueyo A, Tester AM, Pendás AM, Pitiot AS, Astudillo A, Overall CM, Shapiro SD, and López-Otín C (2003). Loss of collagenase-2 confers increased skin tumor susceptibility to male mice. *Nat Genet* **35**, 252–257.

[41] Overall CM and Kleifeld O (2006). Tumour microenvironment—opinion: validating matrix metalloproteinases as drug targets and anti-targets for cancer therapy. *Nat Rev Cancer* **6**, 227–239.

Supplemental Materials and Methods

Immunofluorescence

For immunofluorescence staining of cultivated cells, cells on glass coverslips were fixed and permeated, then incubated with primary antibodies. Fluorescein isothiocyanate– or rhodamine-conjugated secondary antibodies were used to visualize the location of HIF-1α/MT4-MMP. Cell nuclei were counterstained with Hoechst 33342 (Sigma-Aldrich Corp), and fluorescence images were captured using a Leica DMRE epifluorescence microscope (LeiCa TCS SP2, Wetzlar, Germany). For immunofluorescence staining of tumor samples, samples were processed with deparaffinization, rehydration, and antigen retrieval. The subsequent procedures were identical to cellular immunofluorescence. All the antibodies used in immunofluorescence are listed in Table W2.

Table W2. List of Proteins Tested by Antibodies and Characteristics of the Corresponding Antibodies Used.

Protein	Assay	Antibody	Origin	Dilution	Incubation Period
HIF-1α	WB	No. 610959, BD Biosciences	Mouse	1:1000	Overnight, 4°C
HIF-1α	IHC	No. 610959, BD Biosciences	Mouse	1:100	Overnight, 4°C
HIF-1α	IF	No. 610959, BD Biosciences	Mouse	1:100	Overnight, 4°C
MT4-MMP	WB	M3684, Sigma-Aldrich Corp	Rabbit	1:1000	Overnight, 4°C
MT4-MMP	IHC	M3684, Sigma-Aldrich Corp	Rabbit	1:200	Overnight, 4°C
MT4-MMP	IF	M3684, Sigma-Aldrich Corp	Rabbit	1:50	Overnight, 4°C
SLUG	WB	No. 9589, Cell Signaling Technology, Inc	Mouse	1:1000	Overnight, 4°C
SLUG	ChIP	No. 9589, Cell Signaling Technology, Inc	Mouse	1:100	Overnight, 4°C
E-cadherin	WB	No. 4065, Cell Signaling Technology, Inc	Rabbit	1:1000	Overnight, 4°C
N-cadherin	WB	No. 610921, BD Biosciences	Mouse	1:1000	Overnight, 4°C
GAPDH	WB	No. LF-PA0018, Abfrontier Co, Ltd	Rabbit	1:8000	Overnight, 4°C

IF indicates immunofluorescence; *WB*, Western blot.

Cytokine Antibody Arrays

RayBio Human Matrix Metalloproteinase Antibody Array 1 (no. AAH-MMP-1) and RayBio Human Angiogenesis Antibody Array 1 (no. AAH-ANG-1) (RayBiotech, Inc, Norcross, GA) were performed according to the user manual. Briefly, array membranes were incubated for 30 minutes in blocking buffer and then incubated for 2 hours with the conditioned medium collected from SAS-cDNA3 *versus* SAS–MT4-MMP clones. The membranes were washed, and a diluted cocktail of biotinylated antibodies was added for 90 minutes. Membranes were then washed again, and the sandwiched antigens were detected by incubation for 2 hours with a peroxidase-labeled streptavidin solution diluted to 1:1000. Proteins were detected finally by enhanced chemiluminescence, and signals were captured. Array images were quantified with ImageQuant TL software version 5.2 (Amersham Biosciences, Inc., Piscataway, NJ). For each spot, the net density gray level was determined by subtracting the background gray level from the total raw density gray levels. Data after background subtraction were normalized according to positive control densities.

Table W1. Sequence of the Oligonucleotides for siRNA Construct-Making, Real-time PCR, and ChIP Assays.

Assays		Sequence (5′ → 3′)		Amplicon
SiRNA	HIF-1α-si	GATCCCCGAATTCTCAACCACAGTGCTTCAAGAGAG-CACTGTGGTTGAGAATTCTTTTTA		
	MT4-MMP-si	GATCCCCCCCACTTTGACGATGACGATTCAAGAGATCGT-CATCGTCAAAGTGGGTTTTTA		
	SLUG-si	GATCCCCGATGCATATTCGGACCCACTTCAAGA-GAGTGGGTCCGAATATGCATCTTTTTA		
	scramble-si	GATCCCCGTGTCTGTAGGAGTCATCCTTCAAGAGAGGAT-GACTCCTACAGACACTTTTTA		
Real-time PCR	*HIF-1α*	F	AAACTTCTGGATGCTGGTGATTTG	220
		R	TTTCCTCATGGTCACATGGATGA	
	MT4-MMP	F	CTGGGAGTGGAGTGGCTAAGCA	168
		R	TTTCATCAGGGCCAGGGTGG	
	GAPDH	F	AAGGTCGGAGTCAACGGATTTG	149
		R	CCATGGGTGGAATCATATTGGAA	
ChIP	*MT4-MMP* ChIP primer	F	ACACCCGCCCTCGCCCTC	196
		R	CTGACCCTGACTCCCCTCTCCG	
	MT4-MMP control primer	F	TGTTGCTGTGAGACTTGGTCCAG	146
		R	ATCAGGACAACCTGGTTTCCAGA	

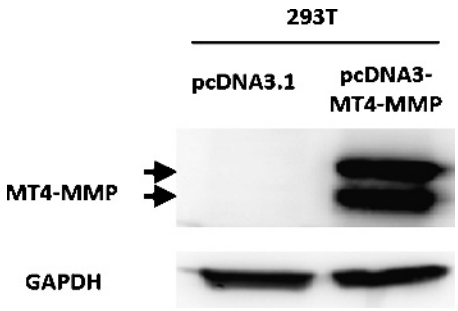

Figure W1. Validation of the efficacy of the constructed MT4-MMP expression vector (pcDNA3–MT4-MMP), specificity of an anti–MT4-MMP antibody used in experiments, and the expression pattern of MT4-MMP protein in Western blot. Western blot analysis of MT4-MMP in 293T cells transfected with pcDNA3–MT4-MMP *versus* pcDNA3.1 empty vector. The Western blot of MT4-MMP revealed two bands (*upper* indicates pro form; *lower*, active form) indicated by black arrows. GAPDH was used as a loading control for the experiment.

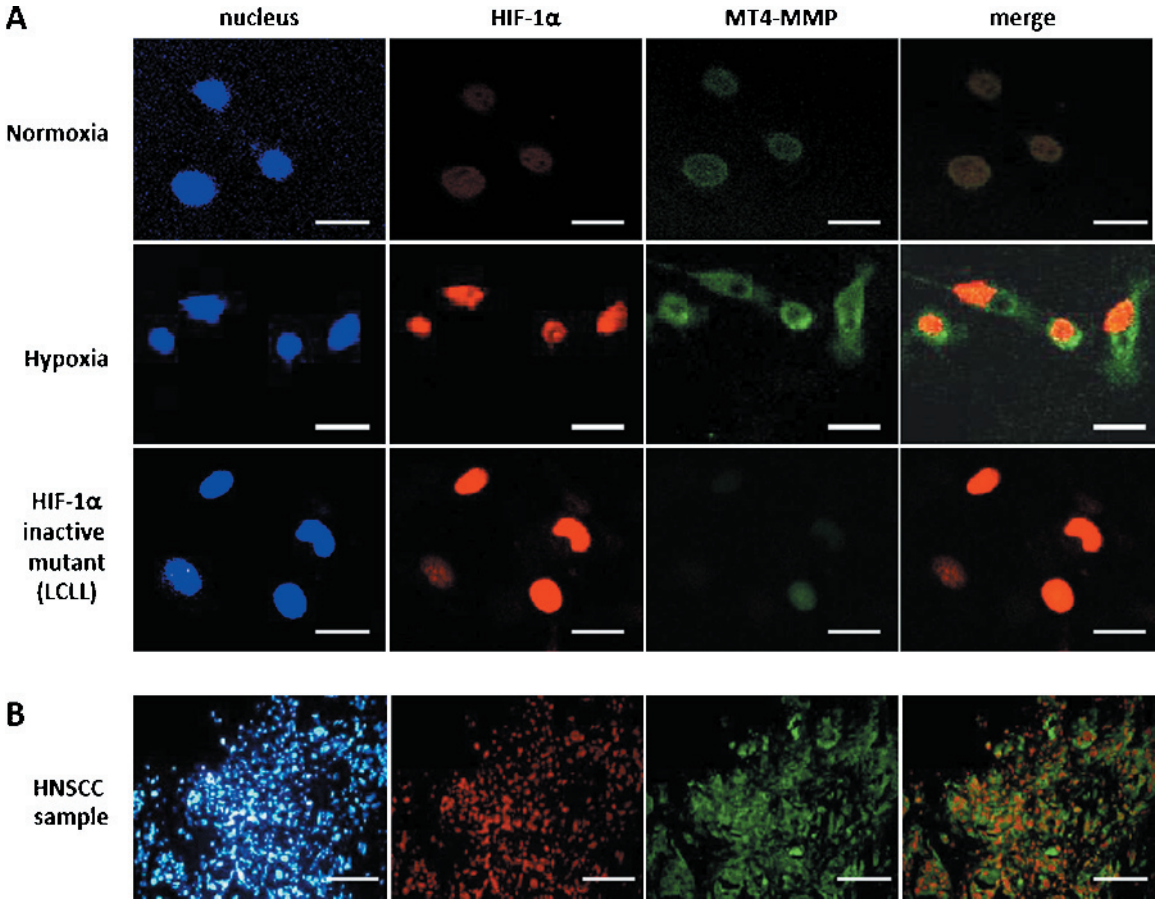

Figure W2. Nuclear expression of HIF-1α promotes membranocytoplasmic expression of MT4-MMP in HNSCC cell lines and samples. (A) Immunofluorescence staining of HIF-1α/MT4-MMP in SAS cells under normoxia (upper panels), hypoxia (middle panels), or expressing inactive HIF-1α mutant (HIF1α(LCLL)) (lower panels). The green signal represented the staining of MT4-MMP, whereas the red signal represented the staining of HIF-1α. The blue signal represented nuclear DNA staining by Hoechst 33342. (B) Immunofluorescence staining of HIF-1α/MT4-MMP in a representative HNSCC case. The green signal represented the staining of MT4-MMP, whereas the red signal represented the staining of HIF-1α. The blue signal represented nuclear DNA staining by Hoechst 33342. Scale bars: A, 20 μm; and B, 200 μm.

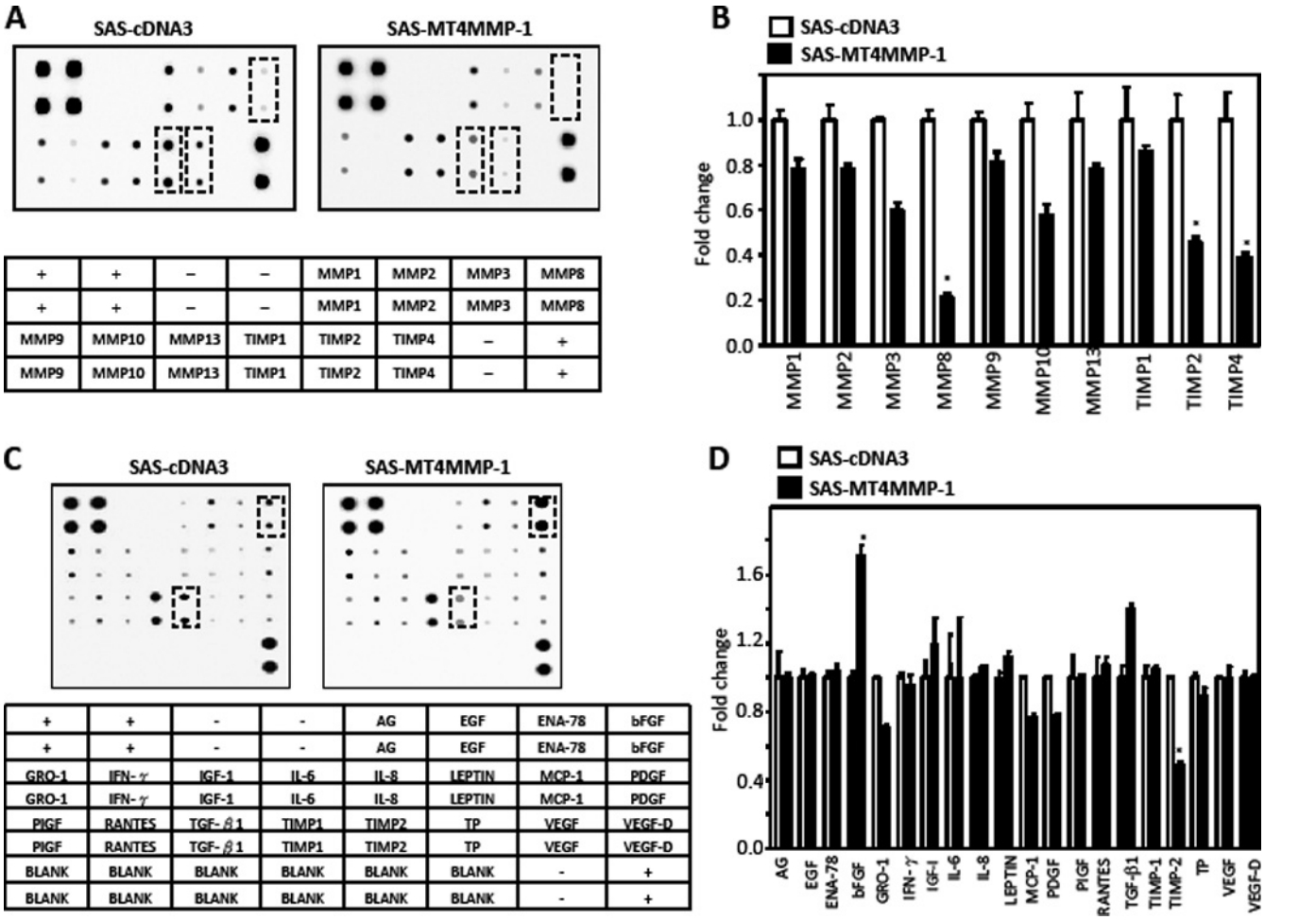

Figure W3. Expression profiles of MMPs and angiogenic proteins in SAS–MT4-MMP *versus* control. (A) Representative picture (upper) with corresponding labeling (lower) of a MMPs array in SAS–MT4-MMP *versus* SAS-cDNA3. The proteins with significant change were circled with broken line. (B) Quantification of protein expression changes in the MMPs array of SAS–MT4-MMP *versus* SAS-cDNA3. (C) Representative picture (upper) with corresponding labeling (lower) of an angiogenic factors array in SAS–MT4-MMP *versus* SAS-cDNA3. The proteins with significant change were circled with broken line. (D) Quantification of protein expression changes in the angiogenic factors array of SAS–MT4-MMP *versus* SAS-cDNA3.

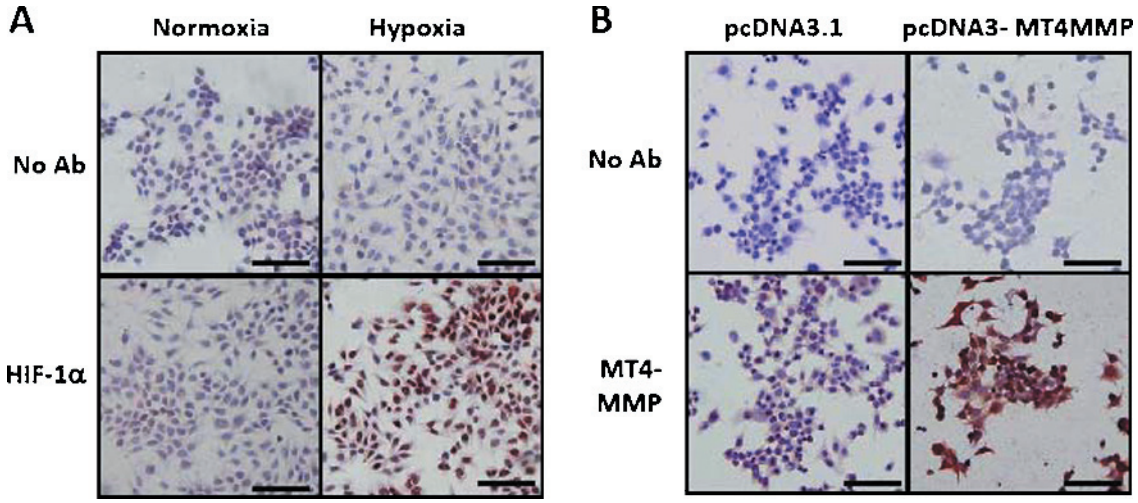

Figure W4. Validation of anti–HIF-1α and anti–MT4-MMP antibodies used in IHC experiments. (A) ICC of HIF-1α in 293T cells under normoxia *versus* hypoxia. No antibody (Ab) was applied as the negative control of ICC experiment. (B) ICC of MT4-MMP in 293T cells transfected with control vector *versus* pcDNA3–MT4-MMP. No Ab was applied as the negative control of ICC experiment. Scale bars, 100 μm.